PAPER

Check for updates

Co$_3$O$_4$/NiO@GQD@SO$_3$H nanocomposite as a superior catalyst for the synthesis of chromenpyrimidines†

Javad Safaei-Ghomi [ID]* and Zahra Omidshafiei

A three-component reaction involving aromatic aldehydes, 6-amino-1,3-dimethyluracil and 4-hydroxycoumarin was achieved in the presence of the Co$_3$O$_4$/NiO@GQD@SO$_3$H nanocomposite as a highly effective heterogeneous catalyst to produce chromenpyrimidines. The catalyst was characterized *via* FT-IR, SEM, XRD, EDS, TGA, BET and VSM. This new catalyst was demonstrated to be highly effective in the preparation of chromenpyrimidines. Atom economy, low catalyst loading, reusable catalyst, applicability to a wide range of substrates and high product yields are some of the important features of this protocol.

1. Introduction

Chromenpyrimidines are a common scaffold in multiple bioactive compounds and possess several pharmacological properties.[1] These compounds are used as analgesic, anti-pyretic,[2] anti-microbial,[3,4] anti-biofilm,[5] anti-inflammatory,[6] anticancer,[7] antitubercular agents.[8] Some other examples of pyrimidines as prominent drug molecules include uramustine, piritrexim isetionate, tegafur, floxuridine, methotrexate, trimethoprim, piromidic acid, tetroxoprim and dipyridamole, which have high bioavailability, slow onset and prolonged effect.[9] Chromenpyrimidines have been regarded as significant targets of organic synthesis. Therefore, the development of effective methods for the preparation of chromenpyrimidines is an attractive challenge. Several methods have been reported for the preparation of chromenpyrimidines in the presence of diverse catalysts including L-proline-derived secondary amino-thiourea,[10] sulfamic acid,[11] Zr(HSO$_4$)$_4$,[12] L-proline,[13] and bifunctional thiourea-based organocatalyst.[14] However, some of the reported procedures have disadvantages including long reaction times, use of toxic and non-reusable catalysts and undesirable reaction conditions. Therefore, to avoid these drawbacks, the search for effective methods for the preparation of chromenpyrimidines is still desirable. Nanoparticles exhibit good catalytic activity owing to their large surface area and active sites. Metal oxides are a broad class of materials that have been researched extensively due to their unique attributes and potential applications in various fields. Graphene quantum

dots (GQDs) are a new member of the carbon nanostructure family, which have quasi-spherical structures. GQDs have gained intensive attention due to their significant features, biological,[15] biomedical,[16] and therapeutic applications,[17] as a new class of photocatalysts[18] and surfactants,[19] and electro-chemical biosensing,[20] electrocatalytic,[21] lithium battery,[22] optical and photovoltaic,[23] photoluminescence,[24,25] bioimaging,[26] and catalytic applications.[27] The potential applications of N-graphene quantum dots were recently reviewed based on experimental and theoretical studies.[28–31] The synthesis of highly efficient nanocomposite catalysts for the synthesis of organic compounds is still a big challenge. To obtain a larger surface area and more active sites, nanocatalysts are function-alized with active groups.[32–34] It has been demonstrated that the decoration of nanocatalysts with GQDs prevents the aggrega-tion of fine particles, and thus increases the effective surface area and number of reactive sites for efficient catalytic reac-tions. The chemical groups on GQD can catalyze chemical reactions, and their –COOH and –SO$_3$H groups can serve as acid catalysts for many reactions.[27–36] Herein, we report the use of a Co$_3$O$_4$/NiO@GQD@SO$_3$H nanocomposite as a new efficient catalyst for the preparation of chromenpyrimidines through a three-component reaction involving aromatic aldehydes, 6-amino-1,3-dimethyluracil and 4-hydroxycoumarin (Scheme 1).

2. Results and discussion

Initially, we prepared Co$_3$O$_4$/NiO nanoparticles *via* simple techniques. A facile hydrothermal method was used for the preparation of N-GQDs.[37] Sulfonated graphene quantum dots were prepared using chlorosulfonic acid.[38] The XRD patterns of Co$_3$O$_4$/NiO, Co$_3$O$_4$/NiO@N-GQDs and Co$_3$O$_4$/NiO@GQD@SO$_3$H nanocomposite are shown in Fig. 1, which confirm the presence of both NiO (JCPDS No.22-1189) and Co$_3$O$_4$ (JCPDS no 65-3103).

Department of Organic Chemistry, Faculty of Chemistry, University of Kashan, Kashan, P. O. Box 87317-51167, I. R. Iran. E-mail: safaei@kashanu.ac.ir; Fax: +98-31-55912397; Tel: +98-31-55912385
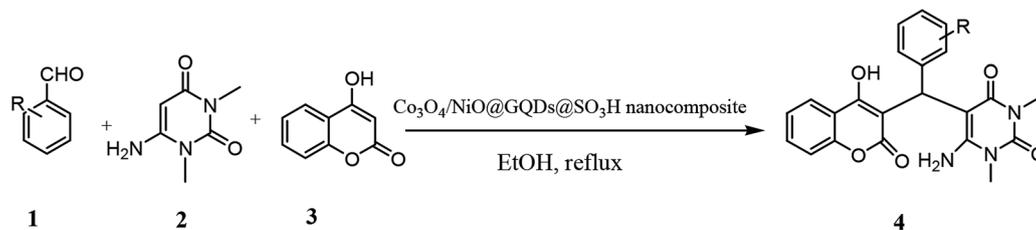
Scheme 1 Synthesis of chromenpyrimidines using the $Co_3O_4/NiO@GQD@SO_3H$ nanocomposite.
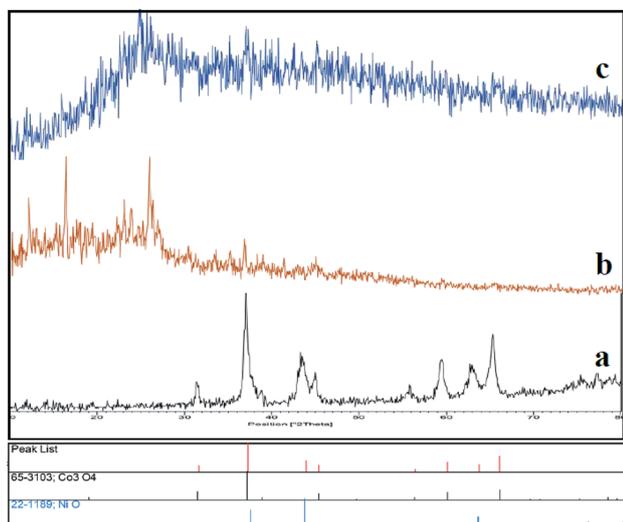
Fig. 1 XRD patterns of (a) Co_3O_4/NiO, (b) $Co_3O_4/NiO@GQDs$ and (c) $Co_3O_4/NiO@GQD@SO_3H$.

To investigate the morphology and particle size of the nanoparticles, SEM images of Co_3O_4/NiO and $Co_3O_4/NiO@GQD@SO_3H$ nanocomposite were measured, as shown in Fig. 2. The SEM images of the $Co_3O_4/NiO@GQD@SO_3H$ nanocomposite show the formation of uniform particles, and the energy-dispersive X-ray spectrum (EDS) confirms the presence of Co, Ni, O, S and C species in the structure of the nanocomposite (Fig. 3).

The magnetic properties of the nanocomposites before and after their decoration with GQDs were tested using a vibrating-sample magnetometer (VSM) (Fig. 4). The lower magnetism of the as-synthesized $Co_3O_4/NiO@GQD@SO_3H$ compared with that of Co_3O_4/NiO is ascribed to the antiferromagnetic behavior of the GQDs as a dopant. These results demonstrate that the magnetization property decreased by coating and functionalization.[39,40]

The FT-IR spectra of Co_3O_4/NiO, $Co_3O_4/NiO@N$-GQD and $Co_3O_4/NiO@GQD@SO_3H$ nanocomposite are shown in Fig. 5. The absorption peak at 3335 cm^{-1} is related to the stretching vibrational absorptions of OH. The peaks at 461.4, 568.4, and 657.1 cm^{-1} correspond to Ni–O, Co^{2+}–O and Co^{3+}–O respectively. The characteristic peaks at 3440 cm^{-1} (O–H stretching
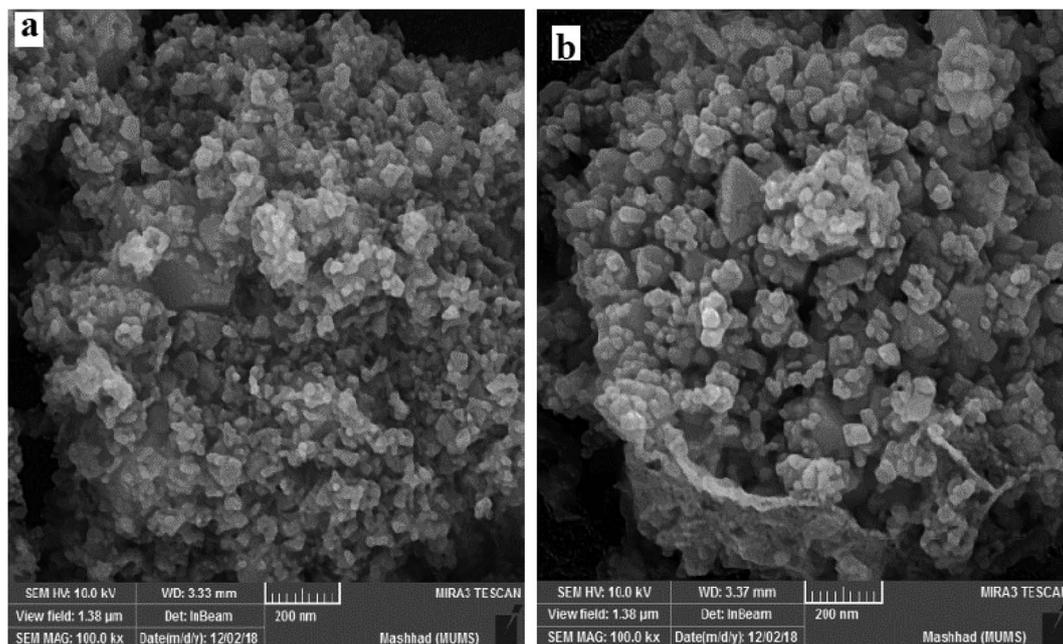
Fig. 2 SEM images of (a) Co_3O_4/NiO and (b) $Co_3O_4/NiO@GQD@SO_3H$.
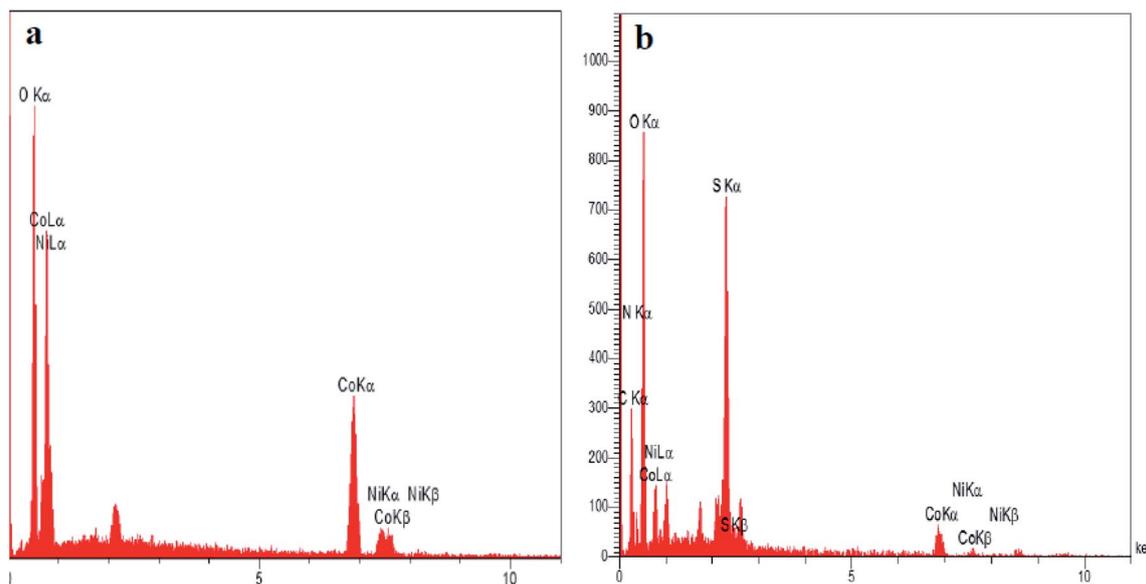
Fig. 3 EDS spectra of (a) Co_3O_4/NiO and (b) $Co_3O_4/NiO@GQD@SO_3H$.

vibration), 1705 cm^{-1} (C=O stretching vibration), and 1125 cm^{-1} (C–O–C stretching vibration) appear in the spectrum in Fig. 5b. The peak at approximately 1475–1580 cm^{-1} is attributed to the C=C bonds. The presence of the sulfonyl group is also verified by the peaks at 1215 and 1120 cm^{-1}. The broad peak at 3350 cm^{-1} is related to the stretching vibrational absorptions of OH (SO$_3$H) (Fig. 5c).

The BET specific surface area of the Co_3O_4/NiO and $Co_3O_4/NiO@GQD@SO_3H$ nanocomposites was measured by nitrogen gas adsorption–desorption isotherms (Fig. 6). The results indicate that the BET specific surface area of Co_3O_4/NiO improved from 12.25 to 32.43 m^2 g^{-1} after modification with the GQDs; therefore, more active sites were introduced on the surface of $Co_3O_4/NiO@GQD@SO_3H$.

TGA (thermogravimetric analysis) was used to evaluate the thermal stability of the $Co_3O_4/NiO@GQD@SO_3H$ nanocomposite. The nanocomposite displayed suitable thermal stability without a significant decrease in weight (Fig. 7). The weight loss at temperatures below 210 °C is owing to the removal of physically adsorbed solvent and surface hydroxyl
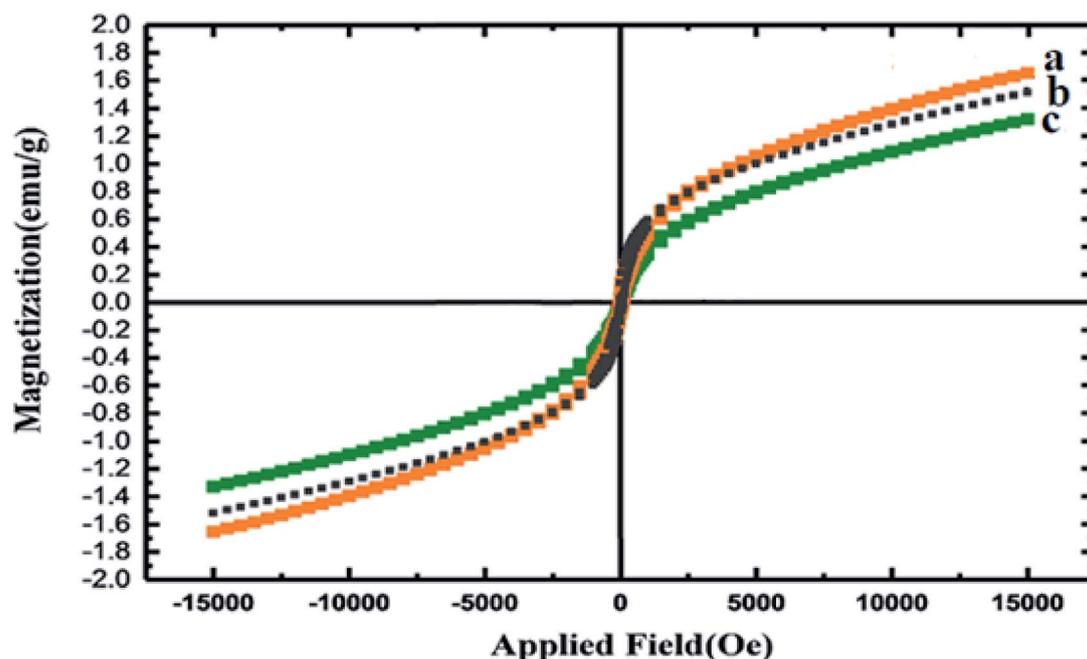

Fig. 4 VSM curves of (a) Co_3O_4/NiO, (b) $Co_3O_4/NiO@GQDs$ and (c) $Co_3O_4/NiO@GQD@SO_3H$.
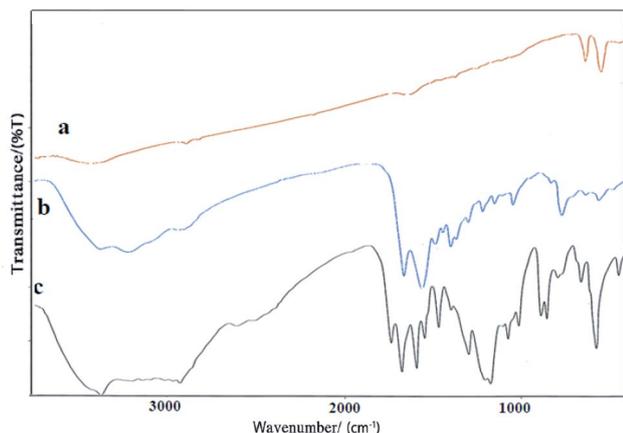
Fig. 5 FT–IR spectra of (a) Co_3O_4/NiO, (b) $Co_3O_4/NiO@GQDs$ and (c) $Co_3O_4/NiO@GQD@SO_3H$.

groups. The curve indicates a weight loss of about 14.06% from 150 °C to 500 °C, which is attributed to the oxidation and degradation of the GQD.

The X-ray photoelectron spectroscopy (XPS) analysis of the $Co_3O_4/NiO@GQD@SO_3H$ nanocomposite is shown in Fig. 8. In the wide-scan spectrum of the nanocatalyst, the predominant components are Ni $2p_{1/2}$ (873.4 eV), Ni $2p_{3/2}$ (854.4 eV), Co $2p_{1/2}$ (792.6 eV), Co $2p_{3/2}$ (780.4 eV), O 1s (529.8 eV), N 1s (400 eV), C 1s (284.5 eV) and S 2p (164.3 eV).

Initially, we carried out a three-component reaction with 4-nitrobenzaldehyde, 6-amino-1,3-dimethyluracil and 4-hydroxycoumarin as a model reaction. The model reactions were performed in the presence of $NaHSO_4$, ZrO_2, p-TSA, Co_3O_4, NiO, Co_3O_4/NiO, $Co_3O_4/NiO@GQDs$ and $Co_3O_4/NiO@GQD@SO_3H$ nanocomposite as catalysts. The reactions were tested using diverse solvents including ethanol, acetonitrile, water and dimethylformamide. The best results were obtained in EtOH and we found that the reaction gave convincing results in the presence of the $Co_3O_4/NiO@GQD@SO_3H$ nanocomposite (5 mg) under reflux conditions (Table 1).

A series of aromatic aldehydes were studied under the optimum conditions (Table 2). Good yields were obtained using

aromatic aldehydes either bearing electron-withdrawing substituents or electron-donating substituents.

We also investigated the recyclability of the $Co_3O_4/NiO@GQD@SO_3H$ nanocomposite as a catalyst for the model reaction under reflux conditions in ethanol. The results showed that nanocomposite can be reused several times without noticeable loss in its catalytic activity (yield in the range of 93% to 91%) (Fig. 9).

The plausible mechanism for the preparation of chromenpyrimidines using the $Co_3O_4/NiO@GQD@SO_3H$ nanocomposite is shown in Scheme 2. Firstly, we assumed that the reaction occurs *via* condensation between 6-amino-1,3-dimethyluracil and aldehyde to form intermediate **I** on the active sites of the $Co_3O_4/NiO@GQD@SO_3H$ nanocatalyst. Then, 4-hydroxycoumarin is added to intermediate **I** to give intermediate **II**. Then, migration of the hydrogen atom provides the final product (Scheme 2).

To study the applicability of this method for large-scale synthesis, we performed selected reactions at the 10 mmol scale. As can be seen, the reactions on a large scale gave the product with a gradual decrease in reaction yield (Table 3).

To compare the efficiency of the $Co_3O_4/NiO@GQD@SO_3H$ nanocomposite with the reported catalysts for the synthesis of chromenpyrimidines, we tabulated the results in Table 4. As indicated in Table 4, the $Co_3O_4/NiO@GQD@SO_3H$ nanocomposite is superior to the reported catalysts. As expected, the increased surface area due to the small particle size increased the reactivity of the catalyst, which is responsible for the accessibility of the substrate molecules on the catalyst surface.

The activity of catalysts is influenced by their acid–base properties and many other factors such as surface area, geometric structure (particularly pore structure), distribution of sites and polarity of the surface sites.[41,42] The SO_3H groups distributed on the surface of $Co_3O_4/NiO@GQDs$ activate the groups of the substrates. In this mechanism, the surface atoms of $Co_3O_4/NiO@GQD@SO_3H$ activate the C=O and C=N groups for better reaction with nucleophiles. The $Co_3O_4/NiO@GQD@SO_3H$ nanocomposite has Lewis and Brønsted acid properties, which increase the activity of the catalyst.
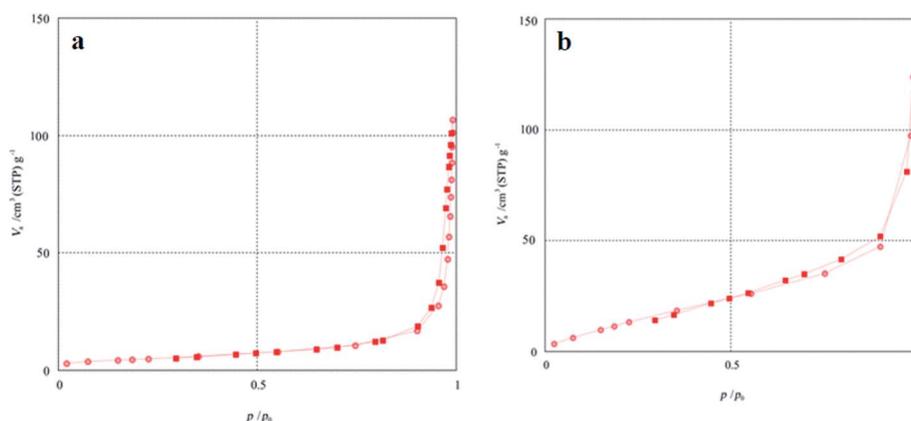

Fig. 6 BET specific surface area of (a) Co_3O_4/NiO and (b) $Co_3O_4/NiO@GQD@SO_3H$.
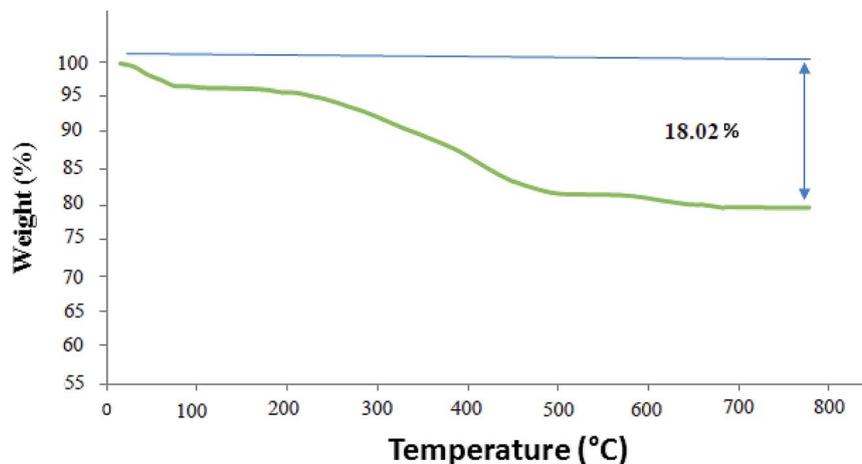
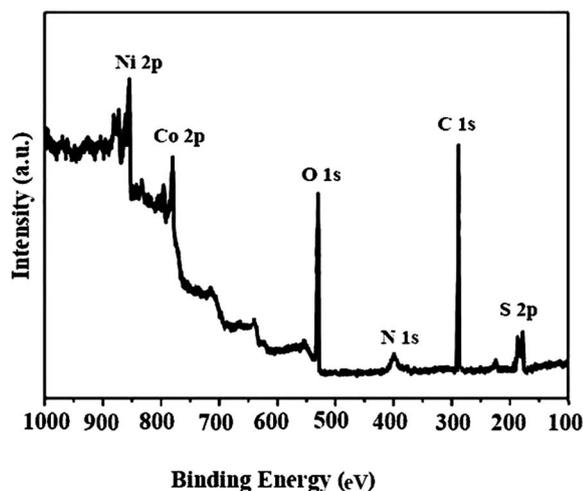**Fig. 7** TGA of Co$_3$O$_4$/NiO@GQD@SO$_3$H nanocomposite.

Fig. 8 X-ray photoelectron spectroscopy (XPS) analysis of the Co$_3$O$_4$/NiO@GQD@SO$_3$H nanocomposite.

3. Experimental

3.1. Chemicals and apparatus

NMR spectra were recorded on a Bruker Avance-400 MHz spectrometer in the presence of tetramethylsilane as an internal standard. IR spectra were recorded on an FT-IR Magna 550 spectrometer using KBr plates. Melting points were determined on an Electrothermal 9200, and are not corrected. Elemental analyses (C, H, and N) were performed on a Carlo ERBA Model EA 1108 analyzer. Powder X-ray diffraction (XRD) was performed on a Philips X'pert diffractometer with monochromatized Cu Kα radiation ($\lambda = 1.5406$ Å). The microscopic morphology of the nanocatalyst was visualized by SEM (MIRA3). Thermogravimetric analysis (TGA) curves were measured on a V5.1A DUPONT 2000. The magnetic measurement of the samples was performed in a vibrating sample magnetometer (VSM) (Meghnatis Daghigh Kavir Co.; Kashan Kavir; Iran).

3.2. Preparation of Co$_3$O$_4$/NiO nanoparticles

Co(NO$_3$)$_3$ and NiCl$_2$ with a 3 : 1 molar ratio were dissolved in ethylene glycol. Afterward, the appropriate amount of aqueous ammonia solution (28 wt%) was added to the above solution until the pH reached 10. Then, the transparent solution was placed in an autoclave at 150 °C for 4 h. The obtained precipitate was washed twice with methanol and dried at 60 °C for 8 h. Finally, the product was calcined at 500 °C for 2 h.

3.3. Preparation of Co$_3$O$_4$/NiO@N-GQD nanocomposite

1 g citric acid and was dissolved in 20 mL deionized water, and stirred to form a clear solution. Subsequently, 0.3 mL ethylenediamine was added to the above solution and mixed to obtain a clear solution. Then, 0.1 g Co$_3$O$_4$/NiO nanoparticles was added to the mixture. The mixture was stirred at room temperature for 5 min. Then the solution was transferred to a 50 mL Teflon-lined stainless autoclave, which was sealed and heated to 180 °C for 12 h in an electric oven. Finally, the as-prepared nanostructured Co$_3$O$_4$/NiO@GQDs was obtained, which was washed several times with deionized water and ethanol, and then dried in an oven until a constant weight was achieved.

3.4. Preparation of Co$_3$O$_4$/NiO@GQD@SO$_3$H nanocomposite

1 g of Co$_3$O$_4$/NiO@N-GQD nanocomposite was dispersed in dry CH$_2$Cl$_2$ (10 mL) and sonicated for 5 min. Then, chlorosulfonic acid (0.8 mL in dry CH$_2$Cl$_2$) was added dropwise to a cooled (ice-bath) mixture of Co$_3$O$_4$/NiO@N-GQDs for 30 min under N$_2$ with vigorous stirring. The mixture was stirred for 120 min, while the residual HCl was removed by suction. The resulted Co$_3$O$_4$/NiO@GQD@SO$_3$H nanocomposite was separated, washed several times with dried CH$_2$Cl$_2$ before drying under vacuum at 60 °C.

3.5. General procedure for the preparation of chromenpyrimidines

A mixture of aldehyde (1 mmol), 6-amino-1,3-dimethyluracil (1 mmol), 4-hydroxycoumarin (1 mmol) and 5 mg Co$_3$O$_4$/

Table 1 Optimization of the reaction conditions using different catalysts[a]
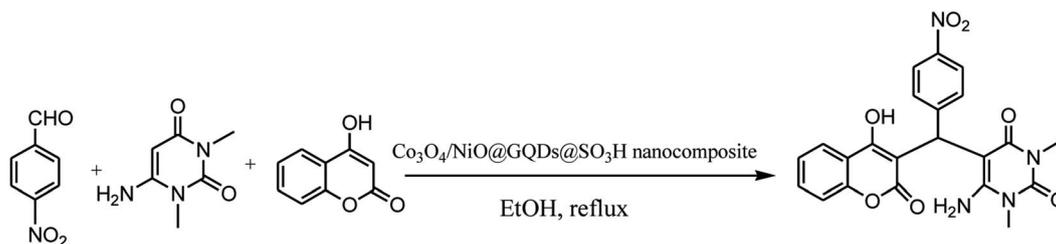
Entry	Catalyst (amount)	Solvent (reflux)	Time (min)	Conversion efficiency	Yield[b] (%)
1	None	EtOH	300	NR	NR
2	Et_3N (5 mol%)	EtOH	300	28	35
3	$NaHSO_4$ (4 mol%)	EtOH	250	37	42
4	ZrO_2 (4 mol%)	EtOH	250	43	48
5	pTSA NPs (5 mol%)	EtOH	250	49	54
6	Nano-Co_3O_4	EtOH	250	40	45
7	Nano-NiO	EtOH	250	45	52
8	Co_3O_4/NiO nanocomposite	EtOH	250	55	60
9	Co_3O_4/NiO@GQD nanocomposite	EtOH	150	68	72
10	Co_3O_4/NiO@GQD@SO_3H nanocomposite (3 mg)	EtOH	80	81	85
11	Co_3O_4/NiO@GQD@SO_3H nanocomposite (5 mg)	EtOH	80	87	93
12	Co_3O_4/NiO@GQD@SO_3H nanocomposite (7 mg)	EtOH	80	87	93
13	Co_3O_4/NiO@GQD@SO_3H nanocomposite (5 mg)	H_2O	100	69	72
14	Co_3O_4/NiO@GQD@SO_3H nanocomposite (5 mg)	DMF	90	71	76
15	Co_3O_4/NiO@GQD@SO_3H nanocomposite (5 mg)	CH_3CN	80	77	82

[a] 4-Nitrobenzaldehyde (1 mmol), 6-amino-1,3-dimethyluracil (1 mmol) and 4-hydroxycoumarin (1 mmol). [b] Isolated yield.

NiO@GQD@SO_3H nanocomposite was stirred in 5 mL ethanol under reflux. The reaction was monitored by TLC. After completion of the reaction, the solution was filtered, and the heterogeneous catalyst was recovered. Water was added, and the precipitate was collected by filtration and washed with water. The crude product was recrystallized or washed with ethanol to give the pure product.

3.6. Spectral data

6-Amino-5-((4-hydroxy-2-oxo-2H-chromen-3-yl)(phenyl) methyl)-1,3-dimethylpyrimidine-2,4(1H,3H)-dione (4a). White solid; m.p. 220–222 °C; IR (KBr): 3432, 3234, 2964, 1695, 1664, 1616, 1569, 1444, 1356, 754 cm^{-1}; ^{1}H NMR (400 MHz, DMSO-d_6) δ: 3.14 (s, 3H, –C$\underline{H}_3$), 3.40 (s, 3H, –C$\underline{H}_3$), 5.62 (s, 1H, –C$\underline{H}$), 7.16–7.85 (m, 11H, Ar$\underline{H}$, –N$\underline{H}_2$), 13.99 (s, 1H, –O$\underline{H}$); ^{13}C NMR (100 MHz, DMSO-d_6) δ: 28.68, 31.02, 36.53, 87.26, 105.11, 116.62, 117.41, 124.17, 124.76, 126.14, 126.80, 128.55, 132.87, 138.74, 150.50, 152.44, 155.63, 164.27, 164.55, 166.27; anal. calcd for $C_{22}H_{19}N_3O_5$: C, 65.18%; H, 4.72%; N, 10.37%. Found: C, 65.20%; H, 4.59%; N, 10.25%.

6-Amino-5-((4-hydroxy-2-oxo-2H-chromen-3-yl)(4-chlorophenyl) methyl)-1,3-dimethylpyrimidine-2,4(1H,3H)-dione (4b). White solid; m.p. 218–220 °C; IR (KBr): 3405, 3211, 2921, 1695, 1663, 1617, 1493, 1448, 763 cm^{-1}; ^{1}H NMR (400 MHz, DMSO-d_6) δ: 3.14 (s, 3H), 3.37 (s, 3H), 5.61 (s, 1H), 7.17–7.85 (m, 10H, ArH and NH$_2$), 13.98 (s, 1H, OH); ^{13}C NMR (100 MHz, DMSO-d_6) δ: 28.72, 31.14, 36.17, 86.98, 104.96, 116.60,

117.35, 124.20, 124.82, 128.43, 128.96, 130.78, 132.96, 138.02, 150.52, 152.40, 155.62, 164.25, 164.52, 166.14; anal. calcd for $C_{22}H_{18}ClN_3O_5$: C, 60.07%; H, 4.12%; N, 9.55%. Found: C, 60.15%; H, 4.18%; N, 9.42%.

6-Amino-5-((4-hydroxy-2-oxo-2H-chromen-3-yl)(4-methoxy phenyl) methyl)-1,3-dimethylpyrimidine-2,4(1H,3H)-dione (4c). Light yellow solid, m.p.: 178–180 °C; IR (KBr): 3413, 3238, 2952, 1695, 1613, 1568, 1508, 1450, 1253, 767 cm^{-1}, ^{1}H NMR (400 MHz, DMSO-d_6) δ: 3.14 (s, 3H), 3.37 (s, 3H), 3.69 (s, 3H), 5.61 (s, 1H), 6.78–6.80 (d, J = 8.0 Hz, 2H), 7.03–7.05 (d, J = 8.0 Hz, 2H), 7.32–7.84 (m, 6H), 13.98 (s, 1H, OH); ^{13}C NMR (100 MHz, DMSO-d_6) δ: 28.66, 31.02, 35.83, 55.43, 87.45, 105.43, 113.95, 116.62, 117.42, 124.15, 124.75, 127.90, 130.32, 132.82, 150.56, 152.42, 155.57, 157.88, 164.20, 164.54, 166.29; anal. calcd for $C_{23}H_{21}N_3O_6$: C, 63.44%; H, 4.86%; N, 9.65%. Found: C, 63.49%; H, 4.74%; N, 9.59%.

6-Amino-5-((4-hydroxy-2-oxo-2H-chromen-3-yl) (4-nitrophenyl) methyl)-1,3-dimethylpyrimidine-2,4(1H,3H)-dione (4d). Light yellow solid; m.p.: 240–242 °C; IR (KBr): 3396, 3210, 2903, 1685, 1619, 1571, 1514, 1346, 769 cm^{-1}; ^{1}H NMR (400 MHz, DMSO-d_6) δ: 3.14 (s, 3H), 3.49 (s, 3H), 5.75 (s, 1H), 7.35–8.10 (m, 10H), 13.96 (s, 1H, OH); ^{13}C NMR (100 MHz, DMSO-d_6) δ: 28.69, 31.05, 36.52, 86.48, 104.72, 117.30, 121.45, 121.63, 124.22, 130.00, 133.04, 134.12, 141.74, 148.41, 150.46, 152.47, 155.80, 164.34, 164.55, 165.98; anal. calcd for $C_{22}H_{18}N_4O_7$: C, 58.67%; H, 4.03%; N, 12.44%; found C, 58.72%; H, 4.09%; N, 12.52%.

Table 2 Synthesis of chromenpyrimidines using the Co_3O_4/NiO@GQD@SO_3H nanocomposite (5 mg) under reflux conditions[a]

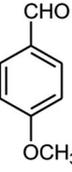| Entry	Aldehyde (1a–1l)	Product	Time (min)	Conversion efficiency	Yield[b] (%)	mp (°C) (ref.)	mp (°C) (reported)
1	CHO	4a	80	80	88	218–220 (10)	220–222
2	CHO (Cl)	4b	80	82	90	219–220 (10)	218–220
3	CHO (OCH_3)	4c	90	72	85	180–181 (10)	178–180
4	CHO (NO_2)	4d	80	87	93	240–242 (13)	240–242
5	CHO (NO_2)	4e	80	80	88	230–232 (10)	230–232
6	CHO (OH)	4f	110	75	83	—	230–232
7	CHO (OH)	4g	100	77	87	—	232–234
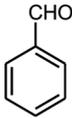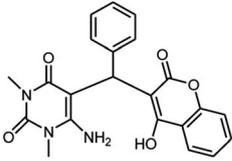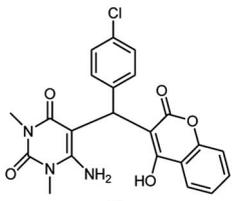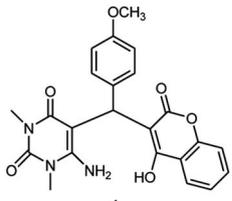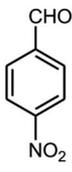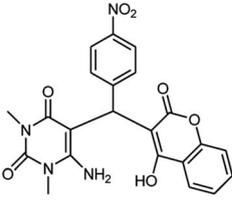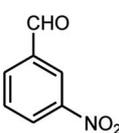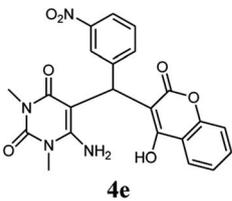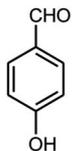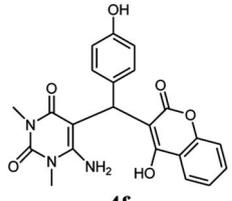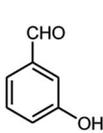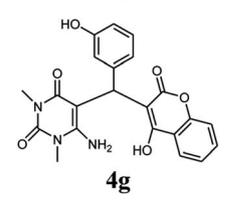
Table 2 (Contd.)

Entry	Aldehyde (1a–1l)	Product	Time (min)	Conversion efficiency	Yield[b] (%)	mp (°C) (ref.)	mp (°C) (reported)
8		**4h**	110	74	81	—	240–242
9		**4i**	90	76	85	202–204 (10)	202–204
10		**4j**	85	80	87	—	200–202
11		**4k**	80	81	89	236–238 (10)	236–238
12		**4l**	100	74	84	257–259 (13)	257–259
13		**4m**	80	79	89	210–212 (10)	210–212
14		**4n**	80	81	88	245–247 (13)	245–247
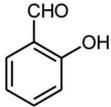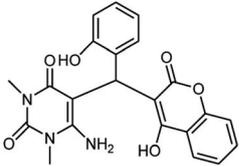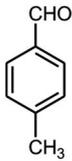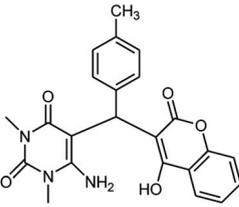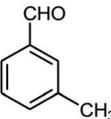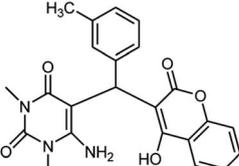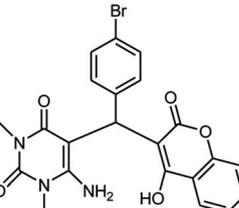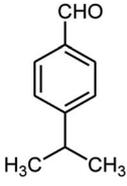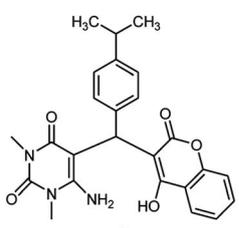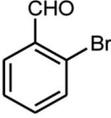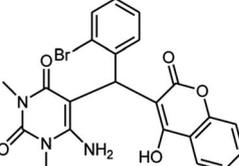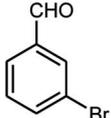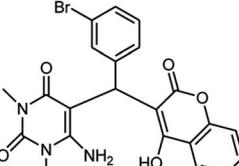
[a] Aromatic aldehydes (1 mmol), 6-amino-1,3-dimethyluracil (1 mmol) and 4-hydroxycoumarin (1 mmol). [b] Isolated yield.
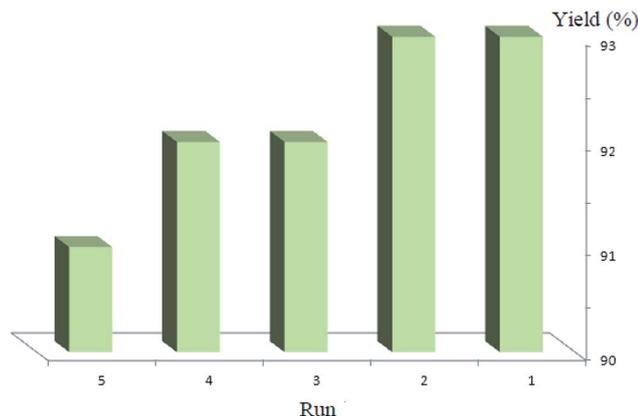
Fig. 9 Recycling of the Co$_3$O$_4$/NiO@GQD@SO$_3$H nanocomposite as a catalyst for the model reaction.

Table 3 The large-scale synthesis of some chromenpyrimidines using the Co$_3$O$_4$/NiO@GQD@SO$_3$H nanocomposite (5 mg)

Entry	Product	Time (min)	Yield^a (%)
1	**4a**	90	86
2	**4c**	95	83
3	**4d**	80	90
4	**4i**	95	82
5	**4k**	80	87

^{a} Isolated yield.

6-Amino-5-((4-hydroxy-2-oxo-2H-chromen-3-yl) (3-nitrophenyl) methyl)-1,3-dimethylpyrimidine-2,4(1H,3H)-dione (4e). Light yellow solid; m.p.: 230–232 °C; IR (KBr): 3460, 3209, 2923, 1699, 1673, 1523, 1437, 1343, 772 cm^{-1}; ^{1}H NMR (400 MHz, DMSO-d_6) δ: 3.14 (s, 3H), 3.38 (s, 3H), 5.76 (s, 1H), 7.36–8.06 (m, 10H), 13.97 (s, 1H, OH); ^{13}C NMR (100 MHz, DMSO-d_6) δ: 28.69, 31.05, 36.52, 86.48, 104.70, 116.54, 117.35, 121.42, 121.62, 124.80, 124.24, 130.14, 133.24, 134.22, 141.75, 148.45, 150.49, 152.42, 155.92, 164.42, 164.45, 165.85; anal. calcd for C$_{22}$H$_{18}$N$_4$O$_7$: C, 58.67%; H, 4.03%; N, 12.44%; found C, 58.75%; H, 4.12%; N, 12.54%.

6-Amino-5-((4-hydroxy-2-oxo-2H-chromen-3-yl) (4-hydroxyphenyl) methyl)-1,3-dimethylpyrimidine-2,4(1H,3H)-dione (4f). White solid; m.p. 230–232 °C; IR (KBr): 3364, 3219, 1695, 1671, 1569, 1509, 1444, 1358, 769 cm^{-1}; ^{1}H NMR (400 MHz, DMSO-d_6) δ: 3.14 (s, 3H), 3.49 (s, 3H), 5.51 (s, 1H), 6.60–6.62 (d, J = 8.0 Hz, 2H), 6.90–6.92 (d, J = 8.0 Hz, 2H), 7.29–7.84 (m, 6H), 9.14 (s, 1H, OH), 13.97 (s, 1H, OH); ^{13}C NMR (100 MHz, DMSO-d_6) δ: 28.64, 30.96, 35.74, 87.54, 105.45, 115.35, 116.55, 117.40, 124.12, 124.73, 127.77, 128.41, 132.79, 150.50, 152.35, 155.43, 155.76, 164.17, 164.49, 166.27. Anal. calcd for C$_{22}$H$_{19}$N$_3$O$_6$: C, 62.70%; H, 4.54%; N, 9.97%; found C, 62.78%; H, 4.59%; N, 10.05%.

6-Amino-5-((4-hydroxy-2-oxo-2H-chromen-3-yl) (3-hydroxyphenyl) methyl)-1,3-dimethylpyrimidine-2,4(1H,3H)-dione (4g). White solid; m.p. 232–234 °C; IR (KBr): 3429, 3306, 2957, 1695, 1670, 1617, 1569, 1447, 1354, 760 cm^{-1}; ^{1}H NMR (400 MHz, DMSO-d_6) δ: 3.15 (s, 3H), 3.38 (s, 3H), 5.55 (s, 1H), 6.53–7.67 (m, 10H), 9.12 (s, 1H, OH), 14.03 (s, 1H, OH); ^{13}C NMR (100 MHz, DMSO-d_6) δ: 28.72, 30.94, 35.72, 87.55, 104.55, 115.34, 116.52, 116.58, 117.42, 124.14, 124.25, 124.78, 127.75, 128.43, 132.79, 151.22, 152.34, 155.42, 155.78, 164.15, 164.45, 166.28. Anal. calcd for C$_{22}$H$_{19}$N$_3$O$_6$: C, 62.70%; H, 4.54%; N, 9.97%; found C, 62.72%; H, 4.55%; N, 10.09%.

6-Amino-5-((4-hydroxy-2-oxo-2H-chromen-3-yl) (2-hydroxyphenyl) methyl)-1,3-dimethylpyrimidine-2,4(1H,3H)-dione (4h). White solid; m.p. 240–242 °C; IR (KBr): 3432, 3306, 2958, 1695, 1607, 1617, 1447, 760 cm^{-1}; ^{1}H NMR (400 MHz, DMSO-d_6) δ: 3.15 (s, 3H), 3.38 (s, 3H), 5.55 (s, 1H), 6.63–7.87 (m,

= Co$_3$O$_4$/NiO@GQDs@SO$_3$H nanocomposite
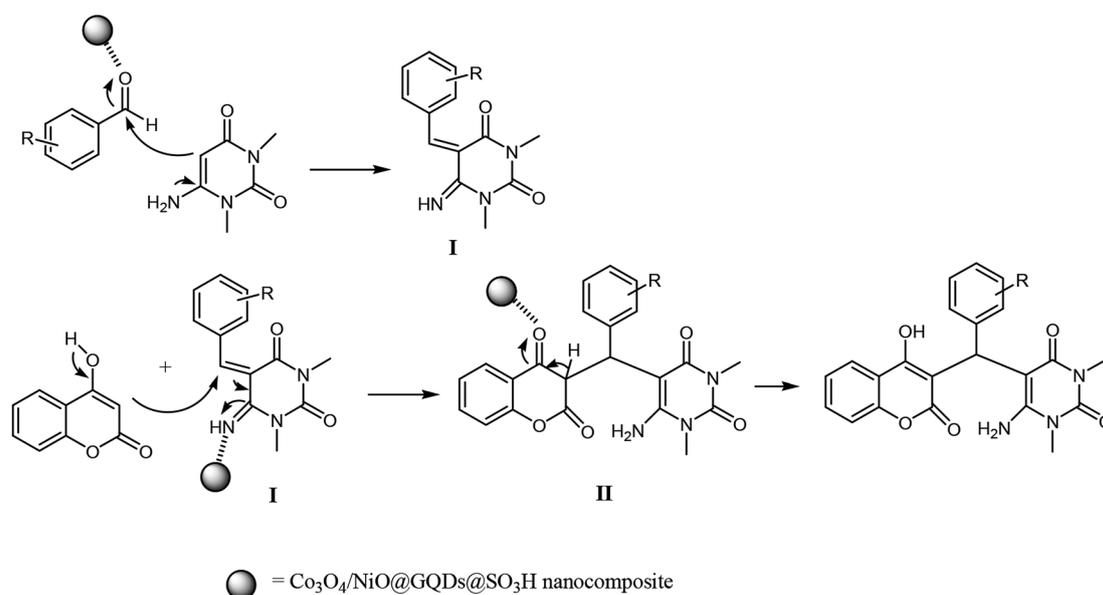
Scheme 2 Proposed mechanism for the three-component reaction.

This journal is © The Royal Society of Chemistry 2019

Table 4 Comparison of the catalytic activity of the $Co_3O_4/NiO@GQD@SO_3H$ nanocomposite (5 mg) with that of other reported catalysts for the synthesis chromenpyrimidines (**4b**)

Entry	Catalyst (conditions)	Time (min)	Conversion efficiency	Yield^a (%)	Ref.
1	L-proline, 20 mol%, EtOH, reflux	360	75	83	13
2	Bifunctional thiourea-based organocatalyst, 20 mol%, H_2O, reflux	240	79	86	14
3	Sulfamic acid, 30 mol%, (EtOH : H_2O: 1 : 1), ultrasound irradiation	30	77	85	11
4	$Co_3O_4/NiO@GQD@SO_3H$ nanocomposite (5 mg, EtOH, reflux)	80	82	90	This work

^{a} Isolated yield.

10H), 9.11 (s, 1H, OH), 14.03 (s, 1H, OH); ^{13}C NMR (100 MHz, DMSO-d_6) δ: 28.67, 31.02, 36.40, 87.35, 104.98, 113.16, 113.69, 116.58, 116.59, 117.48, 124.23, 124.81, 124.83, 129.47, 132.93, 140.27, 150.51, 152.36, 155.52, 157.72, 164.48, 166.23. Anal. calcd for $C_{22}H_{19}N_3O_6$: C, 62.70%; H, 4.54%; N, 9.97%; found C, 62.82%; H, 4.62%; N, 9.98%.

6-Amino-5-((4-hydroxy-2-oxo-2H-chromen-3-yl) (4-methylphenyl) methyl)-1,3-dimethylpyrimidine-2,4(1H,3H)-dione (4i). White solid; m.p. 202–204 °C; IR (KBr): 3411, 3212, 2922, 1697, 1665, 1618, 1569, 1353, 764 cm^{-1}; ^1H NMR (400 MHz, DMSO-d_6) δ: 2.24 (s, 3H), 3.14 (s, 3H), 3.37 (s, 3H), 5.57 (s, 1H), 6.96–7.85 (m, 10H), 13.98 (s, 1H, OH); ^{13}C NMR (100 MHz, DMSO-d_6) δ: 20.60, 28.32, 30.64, 35.74, 87.30, 104.72, 116.25, 123.72, 124.17, 124.42, 126.37, 128.82, 132.58, 134.74, 135.13, 150.18, 152.02, 155.12, 164.15, 165.93, 167.75; anal. calcd for $C_{23}H_{21}N_3O_5$: C, 65.86%; H, 5.05%; N, 10.02%; found C, 65.92%; H, 5.15%; N, 10.08%.

6-Amino-5-((4-hydroxy-2-oxo-2H-chromen-3-yl) (3-methylphenyl) methyl)-1,3-dimethylpyrimidine-2,4(1H,3H)-dione (4j). White solid; m.p. 200–202 °C; IR (KBr): 3403, 3229, 2923, 1699, 1695, 1445, 758 cm^{-1}; ^1H NMR (400 MHz, DMSO-d_6) δ: 2.21 (s, 3H), 3.15 (s, 3H), 3.38 (s, 3H), 5.59 (s, 1H), 6.92–7.86 (m, 10H), 13.97 (s, 1H, OH); ^{13}C NMR (100 MHz, DMSO-d_6) δ: 21.63, 28.66, 30.98, 36.37, 87.34, 105.11, 116.58, 117.37, 123.91, 124.18, 124.77, 126.87, 127.29, 128.42, 132.85, 137.50, 138.66, 150.50, 152.37, 155.52, 164.26, 164.54, 166.25; anal. calcd for $C_{23}H_{21}N_3O_5$: C, 65.86%; H, 5.05%; N, 10.02%; found C, 65.96%; H, 5.18%; N, 10.12%.

6-Amino-5-((4-hydroxy-2-oxo-2H-chromen-3-yl) (4-bromophenyl) methyl)-1,3-dimethylpyrimidine-2,4(1H,3H)-dione (4k). White solid; m.p. 236–238 °C; IR (KBr): 3404, 3212, 2921, 1675, 1663, 1616, 1488, 1446, 761 cm^{-1}; ^1H NMR (400 MHz, DMSO-d_6) δ: 3.13 (s, 3H), 3.37 (s, 3H), 5.58 (s, 1H), 7.11–7.84 (m, 10H), 13.97 (s, 1H, OH); ^{13}C NMR (100 MHz, DMSO-d_6) δ: 28.75, 31.17, 36.19, 86.95, 104.93, 116.63, 117.34, 124.22, 124.85, 128.40, 128.93, 130.79, 132.94, 138.08, 150.55, 152.42, 155.67, 164.28, 164.54, 166.16; anal. calcd for $C_{22}H_{18}BrN_3O_5$: C, 54.56%; H, 3.75%; N, 8.68%. Found: C, 54.62%; H, 3.83%; N, 8.75%.

6-Amino-5-((4-hydroxy-2-oxo-2H-chromen-3-yl) (4-isopropylphenyl) methyl)-1,3-dimethylpyrimidine-2,4(1H,3H)-dione (4l). White solid; m.p. 257–259 °C; IR (KBr): 3463, 3230, 2958, 1695, 1671, 1616, 1569, 1446, 1343, 762 cm^{-1}; ^1H NMR (400 MHz, DMSO-d_6) δ: 1.15 (s, 6H), 2.77 (m, 1H), 3.15

(s, 3H), 3.38 (s, 3H), 5.57 (s, 1H), 7.02–7.85 (m, 10H), 13.99 (s, 1H, OH); ^{13}C NMR (100 MHz, DMSO-d_6) δ: 23.8, 28.1, 30.3, 32.9, 35.6, 87.1, 104.4, 115.8, 116.9, 123.7, 123.9, 125.8, 126.1, 131.9, 135.2, 145.5, 149.9, 151.9, 155.0, 163.8, 164.1, 168.3; anal. calcd for $C_{25}H_{25}N_3O_5$: C, 67.10%; H, 5.63%; N, 9.39%; found C, 67.19%; H, 5.75%; N, 9.45%.

6-Amino-5-((4-hydroxy-2-oxo-2H-chromen-3-yl) (2-bromophenyl) methyl)-1,3-dimethylpyrimidine-2,4(1H,3H)-dione (4m). White solid; m.p. 210–212 °C; IR (KBr): 3402, 3210, 2925, 1676, 1665, 1618, 1489, 1447, 765 cm^{-1}; ^1H NMR (400 MHz, DMSO-d_6) δ: 3.12 (s, 3H), 3.35 (s, 3H), 5.57 (s, 1H), 7.12–7.86 (m, 10H), 13.96 (s, 1H, OH); ^{13}C NMR (100 MHz, DMSO-d_6) δ: 28.74, 31.16, 36.10, 86.94, 104.92, 116.63, 117.29, 124.25, 124.82, 126.35, 127.52, 128.40, 128.92, 130.75, 132.96, 138.05, 150.56, 152.47, 155.65, 164.22, 164.55, 166.14; anal. calcd for $C_{22}H_{18}BrN_3O_5$: C, 54.56%; H, 3.75%; N, 8.68%. Found: C, 54.65%; H, 3.86%; N, 8.77%.

6-Amino-5-((4-hydroxy-2-oxo-2H-chromen-3-yl) (3-bromophenyl) methyl)-1,3-dimethylpyrimidine-2,4(1H,3H)-dione (4n). White solid; m.p. 245–247 °C; IR (KBr): 3405, 3210, 2924, 1673, 1665, 1617, 1489, 1445, 764 cm^{-1}; ^1H NMR (400 MHz, DMSO-d_6) δ: 3.13 (s, 3H), 3.35 (s, 3H), 5.59 (s, 1H), 7.10–7.89 (m, 10H), 13.98 (s, 1H, OH); ^{13}C NMR (100 MHz, DMSO-d_6) δ: 28.74, 31.18, 36.17, 86.95, 104.94, 116.62, 117.31, 124.26, 124.85, 125.33, 126.54, 128.42, 128.94, 130.72, 132.90, 138.07, 150.52, 152.43, 155.64, 164.22, 164.50, 166.12; anal. calcd for $C_{22}H_{18}BrN_3O_5$: C, 54.56%; H, 3.75%; N, 8.68%. Found: C, 54.65%; H, 3.87%; N, 8.79%.

4. Conclusions

In conclusion, we reported an efficient method for the synthesis of chromenpyrimidines using the $Co_3O_4/NiO@GQD@SO_3H$ nanocomposite as a superior catalyst under reflux conditions. The new catalyst was characterized via FT-IR, SEM, XRD, EDS, TGA, BET and VSM. The current method provides obvious advantages, including environmental friendliness, short reaction time, reusability of the catalyst, low catalyst loading and simple workup procedure.

Conflicts of interest

There are no conflicts to declare.

References

1 G. M. Ziarani, N. H. Nasab and N. Lashgari, *RSC Adv.*, 2016, **6**, 38827–38848.
2 R. S. Keri, K. M. Hosamani, R. V. Shingalapur and M. H. Hugar, *Eur. J. Med. Chem.*, 2010, **45**, 2597–2605.
3 U. S. Rai, A. M. Isloor, P. shetty, A. M. Vijesh, N. Prabhu, S. Isloor, M. Thiageeswaran and H. K. Fun, *Eur. J. Med. Chem.*, 2010, **45**, 2695–2699.
4 S. V. Laxmi, B. S. Kuarm and B. Rajitha, *Med. Chem. Res.*, 2013, **22**, 768–774.
5 N. R. Emmadi, K. Atmakur, C. Bingi, N. R. Godumagadda, C. G. Kumar and J. B. Nanubolu, *Bioorg. Med. Chem. Lett.*, 2014, **24**, 485–489.
6 A. A. Abu-Hashem and M. M. Youssef, *Molecules*, 2011, **16**, 1956–1972.
7 C. Sun, C. Chen, S. Xu, J. Wang, Y. Zhu, D. Kong, H. Tao, M. Jin, P. Zheng and W. Zhu, *Bioorg. Med. Chem.*, 2016, **24**, 3862–3869.
8 N. R. Kamdar, D. D. Haveliwala, P. T. Mistry and S. K. Patel, *Med. Chem. Res.*, 2011, **20**, 854–864.
9 T. P. Selvam, C. R. James, P. V. Dniandev and S. K. Valzita, *Res. Pharm.*, 2012, **2**, 01–09.
10 G. Basumatary, R. Mohanta and G. Bez, *Catal. Lett.*, 2019, **149**, 2776–2786.
11 G. Brahmachari, M. Mandal, I. Karmakar, K. Nurjamal and B. Mandal, *ACS Sustainable Chem. Eng.*, 2019, **7**, 6369–6380.
12 S. Abdolmohammadi, S. Balalaie, M. Barari and F. Rominger, *Comb. Chem. High Throughput Screening*, 2013, **16**, 150–159.
13 R. Bharti and T. Parvin, *Synth. Commun.*, 2015, **45**, 1442–1450.
14 R. Bharti and T. Parvin, *RSC Adv.*, 2015, **5**, 66833–66839.
15 X. T. Zheng, A. Ananthanarayanan, K. Q. Luo and P. Chen, *Small*, 2015, **11**(14), 1620–1636.
16 B. Senel, N. Demir, G. Büyükköroglu and M. Yildiz, *Saudi Pharm. J.*, 2019, **27**, 846–858.
17 M. J. Molaei, *RSC Adv.*, 2019, **9**, 6460–6481.
18 T. F. Yeh, C. Y. Teng, S. J. Chen and H. Teng, *Adv. Mater.*, 2014, **26**, 3297–3303.
19 F. Xi, J. Zhao, C. Shen, J. He, J. Chen, Y. Yan, K. Li, J. Liu and P. Chen, *Carbon*, 2019, **153**, 127–135.
20 Y. Wang, Y. Shao, D. W. Matson, J. Li and Y. Lin, *ACS Nano*, 2010, **4**, 1790–1798.
21 Q. Li, S. Zhang, L. Dai and L. S. Li, *J. Am. Chem. Soc.*, 2012, **134**, 18932–18935.
22 A. L. M. Reddy, A. Srivastava, S. R. Gowda, H. Gullapalli, M. Dubey and P. M. Ajayan, *ACS Nano*, 2010, **4**, 6337–6342.
23 M. T. Hasan, R. Gonzalez-Rodriguez, C. Ryan, K. Pota, K. Green, J. L. Coffer and A. V. Naumov, *Nano Res.*, 2019, **12**, 1041–1047.
24 F. Temerov, A. Beliaev, B. Ankudze and T. T. Pakkanen, *J. Lumin.*, 2019, **206**, 403–411.
25 S. Zhu, Y. Song, X. Zhao, J. Shao, J. Zhang and B. Yang, *Nano Res.*, 2015, **8**, 355–381.
26 D. Qu, M. Zheng, J. Li, Z. Xie and Z. Sun, *Light: Sci. Appl.*, 2015, **4**, 364–371.
27 S. Sajjadi, A. Khataee, R. D. C. Soltani and A. Hasanzadeh, *J. Phys. Chem. Solids*, 2019, **127**, 140–150.
28 Y. Du and S. Guo, *Nanoscale*, 2016, **8**, 2532–2543.
29 Y. Yan, J. Gong, J. Chen, Z. Zeng, W. Huang, K. Pu, J. Liu and P. Chen, *Adv. Mater.*, 2019, **31**, 1808283–1808305.
30 M. Li, T. Chen, J. J. Gooding and J. Liu, *ACS Sens.*, 2019, **4**, 1732–1748.
31 Z. Wang, H. Zeng and L. Sun, *J. Mater. Chem. C*, 2015, **3**, 1157–1165.
32 E. Hu, X. Y. Yu, F. Chen, Y. Wu, Y. Hu, X. Wen and D. Lou, *Adv. Energy Mater.*, 2018, **8**, 1702476–1702483.
33 E. Hu, J. Ning, D. Zhao, C. Xu, Y. Lin, Y. Zhong, Z. Zhang, Y. Wang and Y. Hu, *Small*, 2018, **14**, 1704233–1704241.
34 E. Hu, Y. Feng, J. Nai, D. Zhao, Y. Hu, X. Wen and D. Lou, *Energy Environ. Sci.*, 2018, **11**, 872–880.
35 Q. Li, W. Lu, Z. Li, J. Ning, Y. Zhong and Y. Hu, *Chem. Eng. J.*, 2020, **380**, 122544–122552.
36 E. Hu, J. Ning, B. He, Z. Li, C. Zheng, Y. Zhong, Z. Zhang and Y. Hu, *J. Mater. Chem. A*, 2017, **5**, 2271–2279.
37 D. Qu, M. Zheng, P. Du, Y. Zhou, L. Zhang, D. Li, H. Tan, Z. Zhao, Z. Xie and Z. Sun, *Nanoscale*, 2013, **5**, 12272–12277.
38 K. Li, J. Chen, Y. Yan, Y. Min, H. Li, F. Xi, J. Liu and P. Chen, *Carbon*, 2018, **136**, 224–233.
39 N. Limchoowong, P. Sricharoen, Y. Areerob, P. Nuengmatcha, T. Sripakdee, S. Techawongstien and S. Chanthai, *Food Chem.*, 2017, **230**, 388–397.
40 F. Alemi-Tameh, J. Safaei-Ghomi, M. Mahmoudi-Hashemi and R. Teymuri, *Res. Chem. Intermed.*, 2016, **42**, 6391–6406.
41 J. Safaei-Ghomi, H. Shahbazi-Alavi and E. Heidari-Baghbahadorani, *RSC Adv.*, 2014, **4**, 50668–50677.
42 J. Safaei-Ghomi and H. Shahbazi-Alavi, *J. Saudi Chem. Soc.*, 2017, **21**, 698–707.